A novel high-performance low-NO$_x$ fuel-rich/fuel-lean two-stage combustion gas and steam turbine system for power and heat generation

T Yamamoto[1], **N Lior**[*2], **T Furuhata**[3], and **N Arai**[4†]

[1]Department of Mechanical Engineering, Toyohashi University of Technology, Toyohashi, Japan
[2]Department of Mechanical Engineering and Applied Mechanics, University of Pennsylvania, Philadelphia, USA
[3]Department of Mechano-Infomatics and Systems, Nagoya University, Nagoya, Japan
[4]Research Center of Advanced Energy Conversion, Nagoya University, Nagoya, Japan

Abstract: This paper proposes, describes, and analyses a novel high temperature and performance reheat gas turbine (GT) cogeneration system. This newly proposed system employing two-stage fuel-rich and fuel-lean combustion system is named as the 'Fuel Rich–Lean Combustion Reheat GT Cogeneration System' (RLCC). Energy and exergy analyses (the latter mainly to evaluate and demonstrate the reduction in exergy loss of this combustion process compared with conventional single-stage and fuel lean–lean combustion) of the proposed cogeneration system were performed and compared with a conventional cogeneration system. The proposed RLCC system is predicted to have an overall power generation efficiency of up to 53.0 per cent (low heating value (LHV) basis), exergy efficiency up to 61.9 per cent, and specific power up to 524.3 kJ/kg. Compared with a conventional cogeneration (CGC) system, its energy utilization efficiency was as high as 95.0 percent, 4.0 percentage points higher than that of the CGC system, the overall power generation efficiency was higher by 6.2 percentage points, and the exergy efficiency was higher by 7.8 percentage points, and the overall power-based NO$_x$ emissions was reduced by up to 34.0 per cent.

Keywords: gas turbine cogeneration system, exergy analysis, fuel rich–lean staged combustion, low NO$_x$ power generation

1 INTRODUCTION

Gas turbine (GT) cycles are the most widely used in low-to-middle power output cogeneration systems (10–5000 kW) because low capital cost, high flexibility, high reliability without complexity, short delivery times, early commissioning and commercial operation, and fast starting and loading. Furthermore,

their energy utilization efficiencies when used as cogeneration systems can be very high, over 85 per cent, as compared with other energy conversion systems [1]. Cogeneration systems can realize such high efficiencies because of energy cascading, in which high temperature energy is converted to electric power (by means of a combustor and GT) where conversion efficiency is high, and then the waste heat (at low to mid-temperature) is directly used in heating or cooling processes.

Cogeneration systems have, however, low power generation efficiency, typically <35 per cent. The most common route for improving power generation efficiency has been based on increasing the turbine inlet temperature (TIT) up to the metallurgical limit set by the material of turbine blade, but the turbine blades in the low-to-middle power output cogeneration system

Corresponding author: Mechanical Engineering and Applied Mechanics, University of Pennsylvania, 220 South 33d Street, 233 Towne Building, Philadelphia, PA 19104-6315, USA. email: lior@seas.upenn.edu

†*Research center of Advanced Energy Conversion, Nagoya University, Furo-cho, Chikusa-ku, Nagoya, Aichi 464-8603, Japan*

are usually too small to incorporate cooling and thus cannot operate at high TIT of GT power generation plants. As the amount of process steam energy supplied from the cogeneration system is generally larger than that of the thermal energy demand, the combination of the high-energy utilization efficiency with the low power generation efficiency compounds this problem, creating a significant imbalance between the energy demand and supply from the cogeneration system. In response, several approaches have been taken to improve the power generation efficiency, such as steam injection [**2–4**] and humid air turbine (HAT) [**5–9**] systems. Both use water or steam as a part of the working fluid to increase the GT power output. The power generation efficiency of these systems is 2–5 per cent higher than that of conventional cogeneration systems, but one of their drawbacks is the discharge of contaminated water in the exhaust, requiring water drainage and treatment systems, and hence incurring higher operating costs.

The authors have proposed and studied in the past a new concept of a GT system (the 'Chemical Gas Turbine', ChGT) and predicted its feasibility and high efficiency and low NO_x emissions [**10–13**]. The high efficiency is obtained by having a high top inlet temperature, up to and above 2273 K, much higher than the currently used 1723–1773 K, without internal cooling [**14**, **15**], and was made possible by proposing the use of turbine blades made from carbon–fibre-reinforced-carbon (C/C) composites, possibly with thermal barrier coatings, in a reducing environment [**16**, **17**]. Synergistically, that environment also produces low amounts of NO_x. Such conditions are generated by a combination of sequential fuel-rich and fuel-lean combustions: the fuel-rich combustion is found to reduce both the exergy losses in the combustion process and the production of NO_x due to the reduction condition, and whereas the fuel-lean combustion recovers chemical and thermal energies from the fuel-rich combustion. The TIT in the fuel-lean stage is set at about 1623 K that allows the use of conventional GT blades, and the lower temperature also reduces the production of NO_x.

Further, recognizing that C/C composites tend to age rapidly in high temperature oxidizing atmospheres despite their excellent high-temperature resistance, the authors have studied coating techniques of C/C composites, and so far attained more than 10 h of successful operation under high-temperature oxidizing condition [**18**]; further progress is expected to be made at a temperature of 1900 K and O_2 concentration of 21 vol%. From the above-stated studies and considerations, the authors believe that the proposed ChGT system approach is one of the effective ways to improve the low power efficiency of cogeneration systems.

This article thus describes a novel high-performance cogeneration system based on the above-described two-stage combination of high-temperature-fuel-rich and fuel-lean combustion.

2 THE FUEL RICH–LEAN COMBUSTION REHEAT GT COGENERATION SYSTEM

The concept of the new cogeneration system, called 'Fuel Rich–Lean Combustion Reheat GT Cogeneration System (RLCC)', is shown in Fig. 1. This system consists of a fuel-rich combustor (CB1) in series with a downstream fuel-lean combustor (CB2), two associated gas turbines (GT1 and GT2), a recuperator (RE), an intercooler (IC), and a steam generator (SG).

First, air and fuel are compressed by staged compressors with intercooling, and then mixed and burned under fuel-rich (sub-stoichiometric) conditions in CB1. The combustion gas drives the high temperature GT, GT1, having the C/C composites turbine blades, with an inlet temperature above 1773 K. The exhaust gas from the first GT (GT1) still contains chemical energy, possibly as remaining methane, as well as hydrogen and carbon monoxide, which result from the fuel-rich combustion, and is mixed with mid-pressurized air before being burned under fuel-lean conditions in CB2. The exhaust gas from the second combustor drives the second GT (GT2) at lower temperatures at which the construction materials are much less susceptible to oxidation or other deterioration. The GT2 turbine exhaust gas is used to heat the fuel stream and the high- and mid-pressurized air in the recuperator. Finally, the exhaust gas exiting the recuperator is used to generate steam for a back-pressure steam turbine (ST) that produces electric power, as well as process steam at the temperature of 423 K. To respond to thermal or electric energy demand fluctuations in the proposed system, one can control the mass flowrate of extraction steam in the back-pressure ST (stream No. 20 of Fig. 1), and hence the ST power output.

Although fuel preheat such as shown in the recuperator (RE in Fig. 1) is not uncommon in the process and energy industry, there, of course, exists some risk of leakage and ignition that would have to be prevented with proper design. It is noteworthy though that the efficiency drop without this preheat is very small and thus the fuel preheat could be excluded with insignificant deterioration in the performance. Calculations to that effect are shown in section 5.

Since the above-mentioned staged combustion is the key feature of the proposed cogeneration cycle, and since the combustion exergy loss is the single largest loss in fuel-fired power generation systems, the authors begin with an analysis of staged combustion,
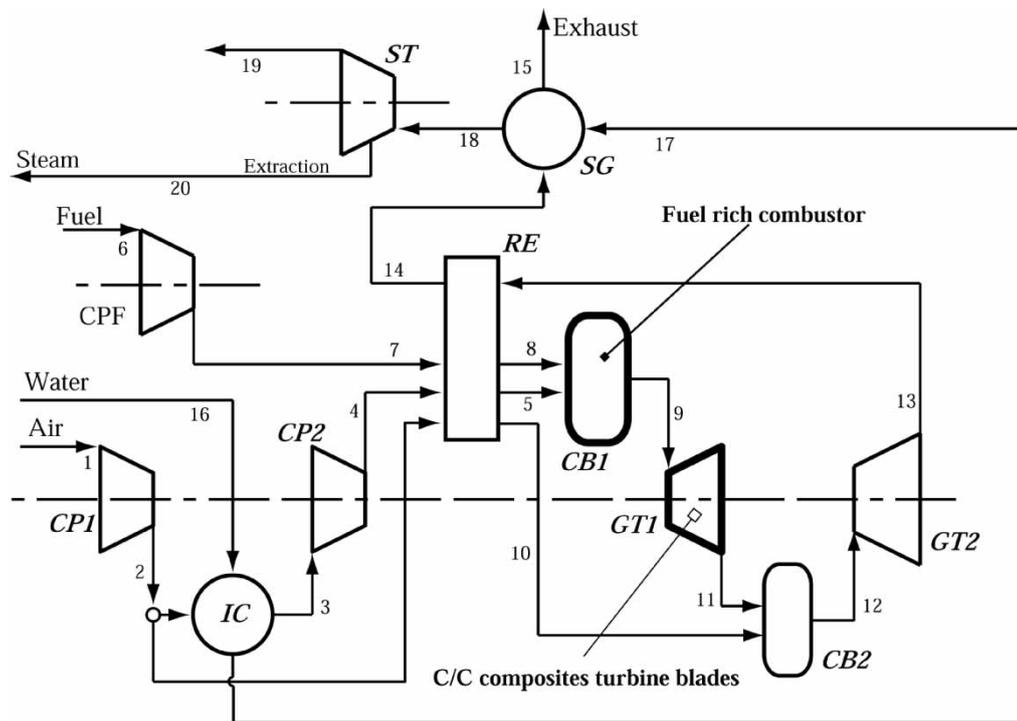
Fig. 1 Flow diagram of the fuel rich–lean combustion reheat gas turbine cogeneration system (RLCC) (CB, combustor; CP, compressor; CG, combustor; GT, gas turbine; IC, intercooler; RE, recuperator; SG, steam generator; ST, steam turbine)

especially the combination of fuel-rich and lean combustion used in this RLCC system, computing power generation efficiency, energy efficiency of utilization, exergy, and exhaust gas emissions in the proposed system, and compared the system with a conventional cogeneration (CGC) system.

3 EXERGY ANALYSIS OF STAGED COMBUSTION SYSTEMS

3.1 Introduction to staged combustion systems

The combustion process dominates the exergy losses in a GT system [**1**, **12**, **13**, **19**–**21**]. It is hence obvious that reductions in combustion exergy losses, as well as increase in the turbine inlet temperature, are desirable for improving the efficiency of GT systems. With these objectives in mind, several staged combustion systems have in the past been proposed and applied to GT cycles. Such systems consist of two combustors: the first combustor burns a part of the fuel and oxidant, and the second combustor is operated using the exhaust gas from the first combustor and the remaining fuel and oxygen. In general, the staged combustion systems described so far operate both combustors under fuel-lean conditions (fuel lean–lean combustion). The ABB ALSTOM company has commercially produced systems GT-24 (180 MW) and

GT-26 (260 MW), which are gas turbines that use a fuel lean–lean combustion system to generate [**22**, **23**].

As described above, the authors propose a different staged combustion concept, with the first combustor operated under fuel-rich conditions using all the fuel and a part of the system's air supply, and the second combustor operated under fuel-lean conditions using the exhaust gas from the first combustor and the remaining air. As indicated, the fuel-rich combustor here produces not only heat, but also fuel (H_2 and CO) for the next combustor.

The governing motivations for the two-stage fuel rich–lean combustion system considered in this article are as follows: (a) the fuel-rich combustion process is a promising method for reducing the exergy loss because it uses much less diluent air, (b) although fuel-rich combustion causes soot formation, such soot formation can be reduced by an internal-recirculation of the fuel-rich combustion exhaust gas containing abundant hydrogen (which inhibits the formation of soot precursors, C2 chemicals) [**24**, **25**], and (c) the fuel-lean combustion stage recovers chemical and heat energies from the fuel-rich combustor, generating very little NO_x because the fuel-lean combustor is operated under the threshold temperature of the Zeldovich NO mechanism, 1773 K, and the formation of the HCN (which is the precursor of the Fenimore NO mechanism) is inhibited in hydrogen and carbon monoxide combustion.

To examine concepts (b) and (c) described above, the authors have constructed fuel-rich and fuel-lean turbulent combustors and experimented with methane as fuel. From the results, it is clear that the hydrogen, the main component of the fuel-rich combustion reaction, reduces soot formation significantly (even though the equivalence ratio of the fuel-rich condition was over 2.0, hardly any soot formed in the experiments) [24, 25], and lowers the NO_x emissions in the fuel-lean combustion below 5 ppm [26].

To explain the features and compare the performances of a conventional staged combustion system with that of the the fuel rich–lean combustion system, an exergy analysis is performed first for both the combustion systems using a simplified combustion reaction model. A single-stage (conventional) combustion system is also analysed for comparison.

3.2 The combustion model

The combustion was composed of two stages, mixing and reaction. To estimate exergy losses in each process, it is assumed that the fuel and oxidant are perfectly mixed in the mixing process, and that the mixed gas completely reacts in the combustion reaction process.

The Gibbs free energy model [27] is used for modelling the combustion reactions. This model is based on the assumption that the exhaust gas from a combustor is in chemical equilibrium, and thus the exhaust gas composition and temperature can be determined by minimizing the Gibbs free energy. The chemicals considered include CH_4, H_2, N_2, O_2, CO, CO_2, and NO_x composed of NO, N_2O and NO_2. Although this model is not strictly correct (for example, the predicted NO_x concentration would be somewhat higher than actual), the results reflect the trends of the actual exhaust gas compositions. It is noteworthy that NO_x and other emissions depend not only on the equivalence ratio and model assumptions, but also critically on the residence time and the flow and transport conditions in the combustion chamber. Precise predictions can thus be made only after the combustor configuration and its operating conditions are selected. Since this is primarily a thermodynamic performance and feasibility study, far preceding the component detailed design phase, this approximate combustion modelling may at least provide rough results and trends.

3.3 Exergy loss in the combustor

The exergy (E) is defined by the equation

$$E = H - T_0 S \tag{1}$$

where T_0 is the 'dead-state' temperature, chosen to be 298 K in this study, H the difference between the gas enthalpy at the existing gas pressure and temperature and at the dead-state pressure and temperature, and S is the difference between the gas entropy at the existing gas conditions and at the dead-state pressure and temperature.

The exergy loss in the mixing process, $E_{loss,mix}$ is the exergy difference between the gases entering and exiting the mixing chamber

$$E_{loss,mix} = E_{mix} - (E_{fuel} + E_{air}) \tag{2}$$

where E_{mix} is the exergy of mixed gas, and E_{fuel} and E_{air} are the exergy of inlet fuel and air, respectively.

The corresponding exergy loss in the reaction process is calculated by

$$E_{loss,burn} = T_0 \cdot [S_{burn}(T_{burn}) - S_{mix}(T_{mix})] \tag{3}$$

where S_{burn} and S_{mix} are the entropy of the combustion products and of the pre-combustion mixture, respectively. The irreversibility of a combustion process is due primarily to the diffusion of the chemical species, the reactions, and inter-molecular heat transfer, with the latter being the dominant, as given in references [19] and [20].

In the following combustion analysis, methane and air (79 vol% N_2, 21 vol% O_2) are used as fuel and oxidant, respectively at inlet temperature and pressure of 298 K and 0.1013 MPa, respectively. The flowrate of the fuel is always set at 1.0 kmol/h (=16.0 kg/h). At this stage, pressure drops are not considerable, so that it is possible for us to isolate and estimate the exergy loss incurred only in the combustion reaction process. These pressure losses are considered further in detail, in the full cycle analyses.

3.4 The single-stage combustion system analysis

A conceptual model of a single-stage combustion system is shown in Fig. 2. In this analysis the flowrate of air (stream No. 2) is adjusted to control the equivalence ratio ϕ of the single-combustion process. ϕ is
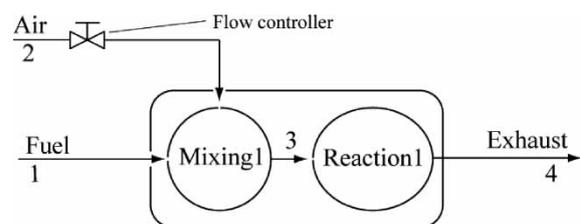
Fig. 2 Schematic diagram of the single-stage combustion system model

defined as

$$\phi = \frac{m_{\text{fuel}}/m_{\text{air}}}{(m_{\text{fuel}}/m_{\text{air}})_{\text{stoich}}} \qquad (4)$$

where $m_{\text{fuel}}/m_{\text{air}}$ denotes the ratio of the mass flowrates of the fuel and the air, and subscript *stoich* denotes the stoichiometric condition.

Figure 3 and Table 1 show the results of the computation of the typical dependence of the combustion temperature (T_4) and relative exergy loss (defined as $E_{\text{loss,burn}}/E_{\text{fuel}}$) on the equivalence ratio ϕ in the process. The combustion relative exergy loss is expressed as a percentage of the fuel exergy value (E_{fuel}). It shows an important characteristic of the process, namely that the combustion exergy loss decreases as the equivalence ratio rises. For $\phi < 1$ (fuel-lean condition), the methane is completely burned, and the combustion products are colder than the temperature at the stoichiometric condition due to the excess air, resulting in a higher relative exergy loss.
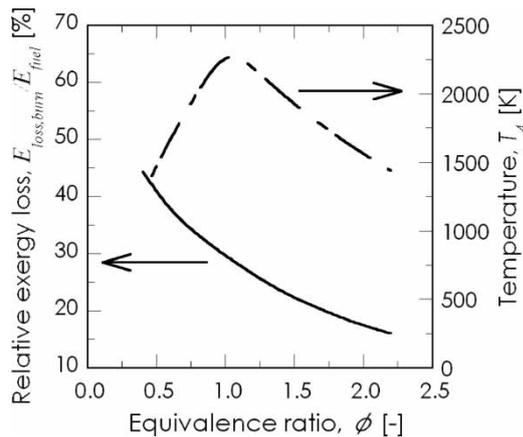
Fig. 3 The effect of the equivalence ratio (ϕ) on the combustion temperature (T_4) and on the relative exergy loss ($E_{\text{loss,burn}}/E_{\text{fuel}}$) for the single-stage combustion model described in Fig. 2 (E_{fuel}, fuel exergy; $E_{\text{loss,burn}}$, combustion exergy loss)

For $\phi > 1$ (fuel-rich condition), not all the methane is burned, with a fraction of its chemical energy converted to thermal energy and the remainder conserved as unburned fuel species such as hydrogen and carbon monoxide, which are exergy rich. Since the ratio of the chemical energy of methane conserved as unburned fuel species increases with ϕ, the exergy loss decreases with ϕ in the fuel-rich condition.

3.5 The staged combustion systems analysis

To simplify the preliminary evaluation of the described two-stage combustion systems, the authors studied two conceptual staged combustion models as shown in Fig. 4: (a) two-stage fuel lean–lean combustion and (b) two-stage fuel rich–lean combustion. To focus on the exergy analysis of the staged combustion, which is of key importance in the overall system, and has never been done before, in this phase of analysis the complexities associated with the internal exergy losses in the gas turbines (such as mechanical and pressure losses, and pressure drops) are eliminated by modelling the turbines as coolers between the combustors. A more detailed modelling of the gas turbines is done further below, when analysing the entire power system. Simplifying the analysis here by modelling some components such as coolers result in more generality, since the simplified model is also applicable to various other industrial components, such as heat exchangers or steam generators.

In this analysis, both the combustion systems employ two flow controllers to control the combustion temperatures of CB1 and CB2. The summary of the assumptions in the two-staged combustion system analysis is shown in Table 2. The computations were performed for the CB1 combustion temperatures (T_5) of 1623, 1773, and 2073 K. The outlet temperature from the cooler and the starting temperature of the second stage (T_6) is always set at 373 K. The combustion temperature in the CB2 (T_9) was set as

Table 1 The conditions and the computed entropy generation and exergy losses in the single-stage combustion (ER, equivalence ratio; E_{fuel}, exergy of the fuel; $E_{\text{loss,burn}}$, exergy loss in the reaction process)

ER, ϕ	Combustion temperature (K)	Air flow, m_{air} (kg/h)	Entropy generation in the fuel–air mixing subprocess, S_{mix} (W/K)	Entropy generation in the combustion reaction subprocess, S_{burn} (W/K)	Relative exergy loss, $E_{\text{loss,burn}}/E_{\text{fuel}}$ (%)
0.4	1272.9	686.9	9.76	321.2	43.1
0.6	1663.6	457.9	9.22	273.6	36.7
0.8	2015.7	343.46	7.99	240.6	32.3
1.0	2256.9	274.8	7.27	214.2	28.7
1.2	2189.2	229.0	7.49	189.8	25.5
1.4	2011.9	196.3	7.08	168.6	22.6
1.6	1847.5	171.7	7.30	151.3	20.3
1.8	1698.8	152.7	6.56	136.8	18.4
2.0	1564.5	137.4	5.97	124.4	16.7
2.2	1438.9	124.9	5.87	113.7	15.3
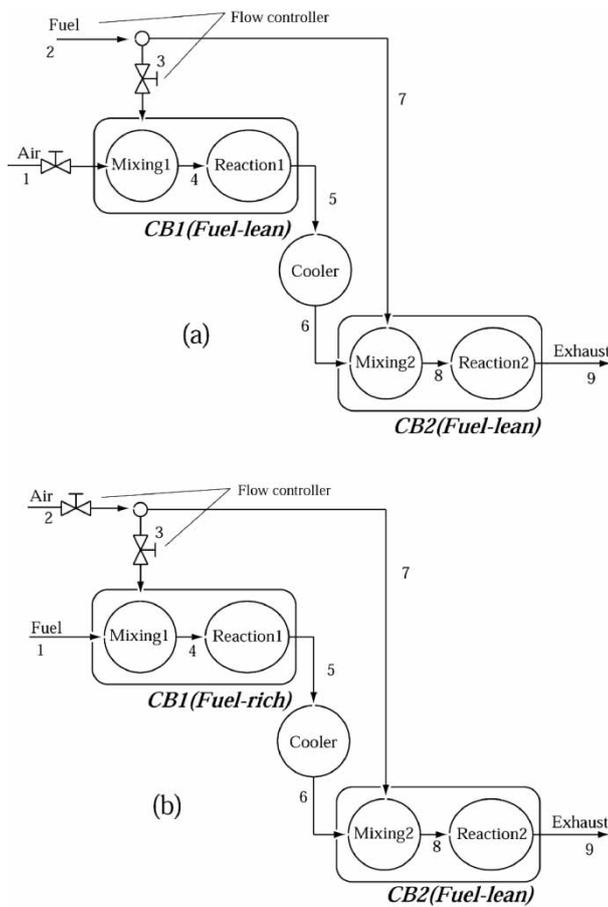
Fig. 4 Schematic diagram of the analysed models of: (a) conventional two-stage (fuel lean–lean) combustion and (b) two-stage fuel rich–lean combustion.

high as possible by controlling the flowrates of stream Nos 2 and 3.

Table 3 shows the results of the exergy analysis and Fig. 5 shows the relative exergy loss components in the two-stage combustion systems described in Fig. 4. Almost all of the exergy loss of the system occurs in the reaction processes of combustors CB1 and CB2. The remaining exergy losses are caused in the mixing

processes in CB1 and CB2, but the former is negligibly small compared with the latter. Considering the effect of equivalence ratio in CB1 (ϕ_{CB1}), the reaction relative exergy loss in CB1 increases as the equivalence ratio is raised in the fuel-lean condition ($\phi_{CB1} \leqslant 1.0$) and it then decreases in the fuel-rich condition ($\phi_{CB1} \leqslant 1.0$) as ϕ_{CB1} is raised further.

Comparing the fuel lean–lean and the fuel rich–lean combustion systems, the exergy loss in the CB1 of the fuel rich–lean combustion system is much lower than that of the fuel lean–lean combustion system. Clearly, there is less air to cool the products down in the CB1 as also seen from the results of the single-stage combustion analysis shown in Table 1 and Fig. 3.

For the same amount of fuel input, the lower exergy loss in the first, fuel-rich, combustor (CB1) of the two-stage fuel rich–lean system allows higher temperature operation of the second, fuel–lean, combustor (CB2) than that in the two-stage fuel lean–lean combustion system. The overall relative exergy loss in the fuel rich–lean combustion system at the combustion temperature of 1623 K is 34.7 per cent, lower by 2.8 percentage points than that in the fuel lean–lean combustion. In addition, it is lower by 2.9 percentage points than that in the single-stage combustion system (37.6 per cent) at the same combustion temperature (Table 1 and Fig. 3). From these results, it can be concluded that the use of two-stage fuel rich–lean combustion not only has the potential to reduce NO_x and offer a reducing environment for the GT1 turbine C/C composites blades, but also to improve efficiency because of the lower exergy loss.

4 ANALYSIS OF THE RLCC SYSTEM

4.1 The simulation model

The RLCC system (Fig. 1) was analysed using the process simulation program HYSYS [**28**]. The exergy values were calculated, using equations (1) to (3), from the HYSYS thermodynamic simulation results that include properties, concentrations, and mass

Table 2 Summary of the main assumptions in the simulation of the two-stage combustion schemes

	Fuel lean–lean combustion			Fuel rich–lean combustion		
No.	Composition	Flowrate	Temperature (K)	Composition	Flowrate	Temperature (K)
1	79 vol% N_2 21 vol% O_2	(Flow control)	$T_0 = 298$	100 vol% CH_4	16.0 kg/h	$T_0 = 298$
2	100 vol% CH_4	16.0 kg/h	$T_0 = 298$	79 vol% N_2 21 vol% O_2	(Flow control)	$T_0 = 298$
3		(Flow control)			(Flow control)	
4						
5			$T_5 = 1623, 1773,$ and 2073			$T_5 = 1623, 1773,$ and 2073
6			$T_6 = 373$			$T_6 = 373$
7						
8						
9	Exhaust			Exhaust		

Table 3 The simulation results for the fuel lean–lean and fuel rich–lean two-stage combustion models (CB1, CB2, first and second combustor; ER, equivalence ratio)

Combustion temperature in CB1 T_5 (K)	Fuel lean–lean combustion			Fuel rich–lean combustion		
	1623	1773	2073	1623	1773	2073
CB1						
ER, ϕ_{CB1}	0.58	0.66	0.84	1.91	1.70	1.33
Fuel/air inflow (kg/h)	9.3/275.6	10.6/274.8	13.4/274.8	16.0/143.9	16.0/161.9	16.0/206.6
Entropy generation in reaction, S_{burn} (W/K)	161.2	173.3	197.0	129.8	143.9	175.5
Exergy loss in CB1 (W)	48 057.4	51 681.1	58 724.5	38 684.4	42 895.5	52 329.2
CB2						
Combustion temperature, T_9 (K)	1287.9	1131.6	777.7	1622.0	1492.9	1090.1
Exhaust gas from CB1/fuel or air flow (kg/h)	284.9/6.7[a]	285.4/5.4[a]	288.2/2.6[a]	159.9/130.9[b]	177.9/112.9[b]	222.6/68.2[b]
Entropy generation in mixing, S_{mix} (W/K)	5.1	5.6	6.7	6.3	5.6	3.9
Entropy generation in reaction, S_{burn}, (W/K)	123.5	107.8	67.0	132.8	121.9	90.4
Exergy loss in CB2 (W)	36 863.0	32 124.6	20 005.5	39 602.1	36 355.7	27 277.5
Total fuel/air flow (kg/h)	16.0/275.6	16.0/274.8	16.0/274.8	16.0/274.8	16.0/274.8	16.0/274.8
Overall ER, ϕ	0.997	1.000	1.000	1.000	1.000	1.000
Exergy loss, E_{loss} (%)	37.5	37.0	35.7	34.7	34.9	35.1

[a] Fuel flow.
[b] Air flow.
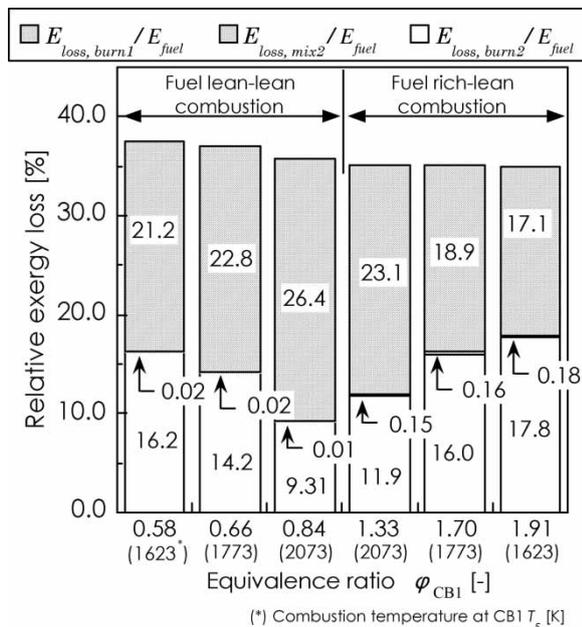
Fig. 5 The relative exergy loss components in the fuel lean–lean and fuel rich–lean two-stage combustion systems for three different temperatures T_5 of the combustor CB1. Note that the number in the middle of each relative exergy-loss bar is the relative exergy loss due to the mixing process in the combustor CB2 (that loss was found to be negligible in CB1) (E_{fuel}, fuel exergy; $E_{loss,burn1}$, combustion exergy loss in the first combustor; $E_{loss,burn2}$, combustion exergy loss in second combustor; $E_{loss,mix2}$, mixing exergy loss in the second combustor)

flows, at each cycle point. A conventional, single-stage CGC, described in Fig. 6, was also modelled and analysed for comparisons with the two-stage combustion advanced system. A summary of the assumptions for
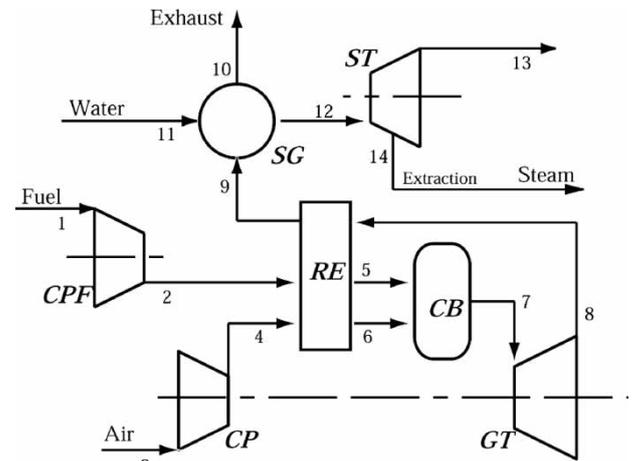
Fig. 6 Flow diagram of the conventional GT cogeneration system, CGC, used for comparison (CP, compressor; CB, combustor; GT, gas turbine; RE, recuperator; SG, steam generator; ST, steam turbine)

the analysis is given in Table 4; all the parameters in Table 4 were kept constant in all the simulations.

It is assumed in the analysis that the compressor and turbine isentropic efficiencies are 85 per cent, and that the pressure drop in each component is 3 per cent of its inlet pressure. The ambient air was assumed to be dry, at 298 K, 0.1013 MPa, and the fuel was methane with a lower heating value of 50.01 kJ/kg, supplied at ambient pressure at a mass flowrate of 383.5 kg/h, for a total heat input of 19.2 MJ/h. The top inlet temperature of the first GT (TIT1 of GT1) was controlled by the equivalence ratio at CB1, and TIT2 (the TIT of GT2) is set at 1723 K by regulating a cooling air flow (stream No. 10 in Fig. 1). The heat recovery steam generating system uses two heat exchangers, SG and IC. The inlet feed water to this system was assumed to be at

Table 4 Summary of the main assumptions used in all the simulations of the RLCC system

Stream no.	Composition	Flowrate	Temperature (K)	Pressure (MPa)
1	79 vol% nitrogen 21 vol% oxygen		T_0 (298)	$P_0 = 0.1013$
2				
3				
4				(Table 5)
5			$T_5 = T_8 = T_{10} = 773$	
6	100 vol% methane	383.45 kg/h	$T_0 = 298$	
7				
8				
9			(Table 5)	
10				$P_{10} = P_{11}$
11				$P_{10} = P_{11}$
12			1623	
13				
14				
15			348	
16	100 vol% water		298	5.0650
17				
18				
19				0.1013
20	Steam		423	0.5065

298 K, 5.0 MPa. The pinch point temperature difference between the hot and cold streams in each heat exchanger was assumed to be 15 K, and it is assumed that there are no heat losses from the heat exchangers.

The focus of this analysis was to determine the influences of the top pressure (TP) and TIT1 on system performance, and to find the conditions for optimal performance. The analysis was conducted by running simulations for different combinations of the RLCC parameter values listed in Table 5. This table also indicates the equivalence ratios at each combustor. All the results were compared with the conventional cogeneration systems (CGC, Fig. 6 and Table 6).

Table 5 The parameter values varied in the simulation runs of the RLCC system (CB1, first combustor; TIT1, turbine inlet temperature of first GT)

TIT1 (stream no. 9) (K)	Top pressure (stream no. 4), TP (MPa)	Equivalence ratio in CB1, ϕ_{CB1}
1623	2.0, 3.0, 4.0	2.51
1673		2.43
1773		2.27
2073		1.86

Table 6 Parameter values for the CGC system (CB, combustor; TIT, turbine inlet temperature)

TIT (K)	Top pressure (stream no. 7), TP (MPa)	Equivalence ratio in CB, ϕ_{CB}
1623	2.0	0.39
	3.0	0.36
	4.0	0.34
1673	2.0	0.42
	3.0	0.39
	4.0	0.36
1773	2.0	0.46
	3.0	0.44
	4.0	0.41

4.2 The exergy loss in the gas turbines, compressors, pumps, and steam turbine

The exergy losses are calculated by the equation

$$|E_{in} - E_{out}| = E_{loss} + |E_{GT,ST,CP}| \qquad (5)$$

where subscripts 'in' and 'out' represent the inlet and outlet conditions at each component, and $E_{GT,ST,CP}$ is the exergy of the gas or (ST) output or compressor and pump input, respectively.

4.3 System performance criteria

To achieve high power generation efficiency of this cogeneration system, the topping GT cycle must have high efficiency because the steam bottoming cycle supplies not only electricity but also heat, and the power it generates is varied during operation to respond the varying demands of electricity and heat. Consequently, two performance criteria are defined to evaluate the topping GT cycle, power generation efficiency, η_{GT-pow}, and specific power, SP

$$\eta_{GT-pow} = (W_{GT} - W_{CP})/Q_{fuel} \qquad (6)$$
$$SP = (W_{GT} - W_{CP})/(m_{air} + m_{fuel}) \qquad (7)$$

where $(m_{air} + m_{fuel})$ is the sum of the mass flowrates of the air and fuel, and Q_{fuel} is the low heating value of the fuel.

Next, GT and ST power generation performances using overall power generation efficiency, η_{pow} are evaluated

$$\eta_{pow} = (W_{GT} + W_{ST} - W_{CP})/Q_{fuel} \qquad (8)$$

and finally the overall system performances including power and heat generations via its energy and exergy

efficiencies, η_{util}, and η_{ex}, respectively, are analysed

$$\eta_{ex} = (E_{GT} + E_{ST} - E_{CP} + E_{heat})/E_{fuel} \qquad (9)$$

$$\eta_{util} = (E_{GT} + E_{ST} - E_{CP} + Q_{heat})/Q_{fuel} \qquad (10)$$

where Q_{heat} is the amount of steam heat supplied by the steam bottoming cycle (stream no. 20 in Fig. 1).

5 RESULTS OF THE SYSTEM ANALYSIS AND DISCUSSION

Tables 7 and 8 show the major performance results of the CGC and of the proposed systems, respectively. These results were calculated for the condition of maximal ST power generation, then extraction streams from ST (stream No. 20 in Fig. 1, and No. 14 in Fig. 6) are set to zero value. Although the ST power output (W_{ST}) and exhaust gas flowrate (stream No. 15 in Fig. 1) in the RLCC system are smaller than those in the CGC system, its overall power generation efficiency, η_{pow}, is ~6.4 percentage points higher than

that in the CGC system under the same conditions (TIT = TIT1 = 1623 K, TP = 2.0 MPa). In the considered range of parameters, the RLCC system produces the highest overall power generation efficiency, of over 53.0 per cent, at TIT1 = 2073 K and TP = 4.0 MPa, which is 6.5 percentage points higher than that of the CGC system at TIT = 1773 K and TP = 2.0 MPa. This is mainly attributable to the performance of the topping GT cycle rather than that of the bottoming ST cycle.

Figure 7 shows performance charts (the relationship between the power generation efficiency, η_{GT-pow}, and specific power, SP) of the topping GT cycles of the RLCC and the CGC systems. In the RLCC system, the highest power generation efficiency $\eta_{GT-pow} = 40.5$ per cent and specific power SP = 518.7 kJ/kg are found at TIT1 = 1773 K and TP = 4.0 MPa. The CGC system shows the highest power generation efficiency $\eta_{GT-pow} = 30.8$ per cent at TIT = 1773 K and TP = 4.0 MPa, and the highest specific power SP = 406.2 kJ/kg at TIT = 1773 K and TP = 2.0 MPa. The results indicate that the fuel rich-lean combustion system has: (a) a high power generation efficiency

Table 7 The major performance results of the CGC system, TIT = 1623 K (m_{air}, m_{fuel}, mass flowrate of the air and fuel; SP, specific power; TIT, turbine inlet temperature; TP, top pressure of the system; W_{CP}, compressor work; W_{GT}, GT power compressor work; W_{ST}, ST power; η_{GT-pow}, power generation efficiency of topping GT cycle; η_{pow}, overall power generation efficiency)

TIT (K)	TP (MPa)	W_{GP} (kW)	W_{CP} (kW)	W_{ST} (kW)	$m_{air} + m_{fuel}$ (kg/hr)	η_{GT-pow} (%)	η_{pow} (%)	SP (kJ/kg)
1623	2.0	3824.1	2307.1	849.9	17 197.2	28.5	44.4	317.6
	3.0	4231.2	2618.2	832.2	18 589.8	27.7	43.6	360.4
	4.0	5070.4	3676.3	859.3	19 979.6	26.2	42.3	251.2
1673	2.0	3737.7	2176.1	845.5	16 208.3	29.3	45.2	346.9
	3.0	4346.8	2815.7	844.4	17 345.3	28.7	44.6	317.8
	4.0	4912.2	3436.3	848.2	18 662.0	27.7	43.6	284.7
1773	2.0	3591.1	1952.8	837.8	14 521.4	30.76	46.5	406.2
	3.0	4148.0	2509.1	830.6	15 433.4	30.8	46.4	382.3
	4.0	4650.4	3037.7	829.1	16 473.4	30.3	45.8	352.4

Table 8 The major performance results of the RLCC system (m_{air}, m_{fuel}, mass flowrate of the air and fuel; SP, specific power; TIT1, turbine inlet temperature of the first GT; TP, top pressure of the system; W_{CP1}, W_{CP2}, first and second compressor work; W_{GT1}, W_{GT2}, first and second GT power; W_{ST}, ST power; η_{GT-pow}, power generation efficiency of topping GT cycle; η_{pow}, overall power generation efficiency)

TIT1 (K)	TP (MPa)	MP (MPa)	W_{GT1} (kW)	W_{GT2} (kW)	$W_{CP1} + W_{CP2}$ (kW)	W_{ST} (kW)	$m_{air} + m_{fuel}$ (kg/h)	η_{GT-pow} (%)	η_{pow} (%)	SP (kJ/kg)
1623	2.0	0.8	375.9	3041.4	1459.7	737.6	16 694.3	36.8	50.6	422.1
	3.0	1.0	443.4	3211.4	1643.1	717.4	16 245.1	37.8	51.2	445.8
	4.0	1.0	541.0	3165.7	1664.1	710.7	16 006.8	38.3	51.7	459.4
1673	2.0	0.8	394.2	3029.7	1457.3	733.8	16 628.6	36.9	50.7	425.8
	3.0	1	465.1	3193.6	1638.2	713.4	16 152.1	37.9	51.3	450.3
	4.0	1	567.4	3147.6	1660.2	705.9	15 912.3	38.6	51.8	464.9
1773	2.0	0.8	432.4	3005.4	1452.3	725.8	16 491.3	37.3	50.9	433.4
	3.0	0.8	465.1	3193.6	1638.2	713.4	16 152.1	37.9	51.3	450.3
	4.0	1	622.6	3109.7	1651.9	695.8	15 715.1	39.1	52.1	476.6
2073	2.0	0.8	561.7	2899.1	1425.0	702.6	15 891.5	38.2	51.4	461.2
	3.0	0.8	773.3	2772.7	1441.5	688.2	15 177.7	39.5	52.4	499.2
	4.0	1	807.6	2968.8	1617.9	664.3	14 980.7	40.5	53.0	518.7
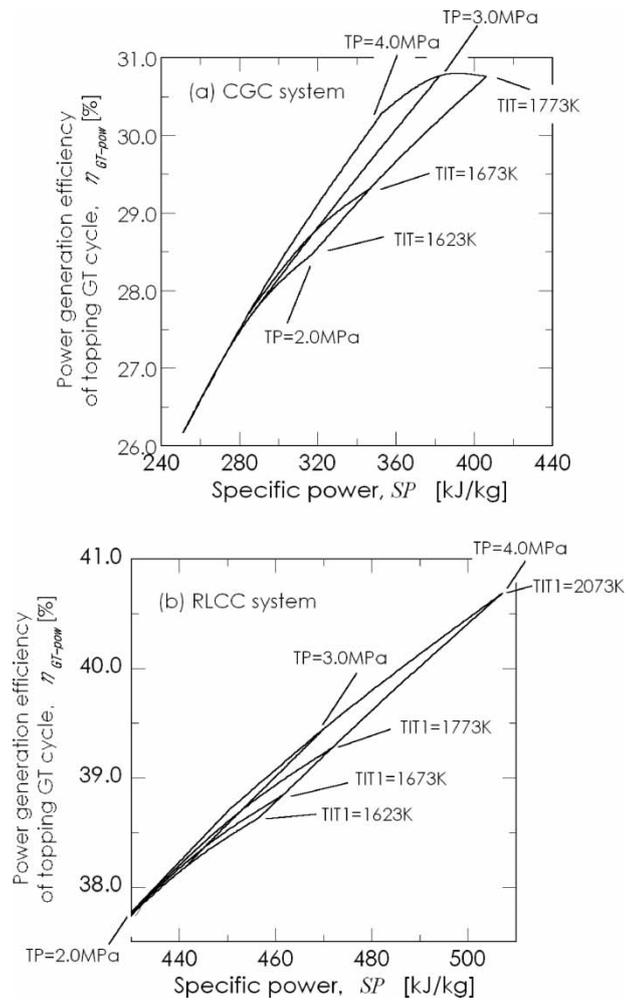
Fig. 7 Performance charts of cogeneration systems: (a) the CGC system and (b) the RLCC system (TP, top pressure of the system; TIT, turbine inlet temperature)

of the topping GT cycle $\eta_{\text{GT-pow}}$, and consequently, a higher overall power generation efficiency η_{pow} (the details are addressed in the following section) and (b) a higher specific power of topping GT cycle SP, than the reference CGC.

Figures 8(a) and (b) show the exergy distribution diagrams of the CGC and RLCC systems when TIT and TIT1 are set to 1623 K, respectively. The values in these figures show the exergy proportions relative to the input exergy of the fuel taken as 100%. For the proposed RLCC system, the exergetic efficiency of power generation alone was found to be 47.5 per cent, and the exergy efficiency of the entire cogeneration system, η_{ex} (equation (9)) 59.8 per cent, almost 7.8 percentage points higher than those of the CGC system. The exergy loss in both of the combustors (CB1 and CB2) in the RLCC system is lower by 1 percentage point than that of the CGC system. The reason for this exergy loss reduction is that the combination of
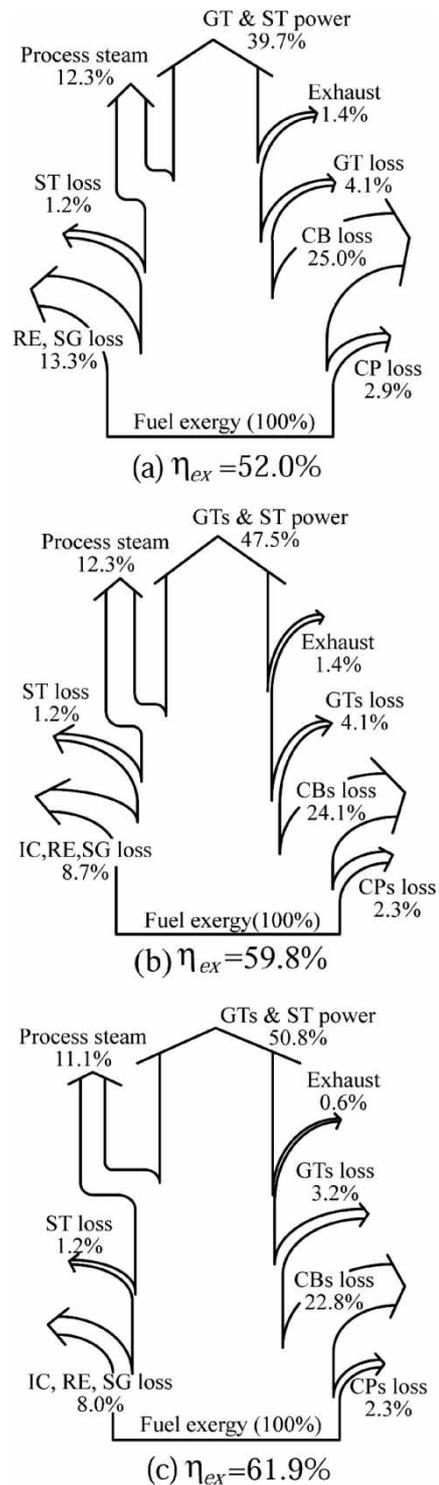
Fig. 8 Exergy flow diagrams of: (a) the CGC system, TIT = 1623 K, TP = 2.0 MPa, and r_{HE} = 1.15, (b) the RLCC system, TIT1 = 1623, TP = 2.0 MPa, MP = 0.8 MPa, and r_{HE} = 1.02, and (c) the RLCC system, TIT1 = 2073, TP = 2.0 MPa, MP = 0.8 MPa, and r_{HE} = 0.91 (CB, combustor; CP, compressor; GT, gas turbine; IC, intercooler; RE, recuperator; SG, steam generator; ST, steam turbine)

fuel-rich and-lean combustion produces a reduction of exergy loss in combustion as shown in the previous section. Also, the exergy loss due to the heat exchange processes such as in the heat exchangers SG, RE, and IC, is 5 percentage points smaller than that in the CGC.

Figure 8(c) is the exergy distribution diagram of the RLCC system when TIT1 is set at 2073 K. Comparison of the RLCC system performance for the different TIT1 values (1623 K and 2073 K) shows three important consequences of increasing the TIT1 in the proposed system: the combustion exergy loss is reduced by 1.3 percentage points, the power generation exergetic efficiency is increased by 2.8 percentage points, and the amount of process steam heat is reduced by 1.2 percentage points.

Figure 9 shows the dependence of the overall power generation efficiency η_{pow} and energy efficiency of utilization η_{util}, on the heat-to-electricity generation ratio r_{HE}, defined as

$$r_{HE} = Q_{heat} / (W_{GT-s} + W_{ST} - W_{CP-s}) \qquad (11)$$

To generate the results shown in Fig. 9, r_{HE} was varied by controlling the steam extraction flowrate at the ST (stream No. 20 in Fig. 1, and No. 14 in Fig. 6), and top pressure TP and turbine inlet temperatures (TIT1 of RLCC and TIT of CGC) are kept at 2.0 MPa and 1723 K, respectively. Increasing the heat-to-electricity generation ratio, r_{HE}, is seen to decrease the power generation efficiency (η_{pow}), but to increase the energy utilization efficiency (η_{util}), for both the CGC and RLCC systems. The energy utilization efficiency η_{util} of the RLCC system is 5.0 percentage points higher than that of the CGC system for all r_{HE}, because the overall power generation efficiency of the RLCC system is
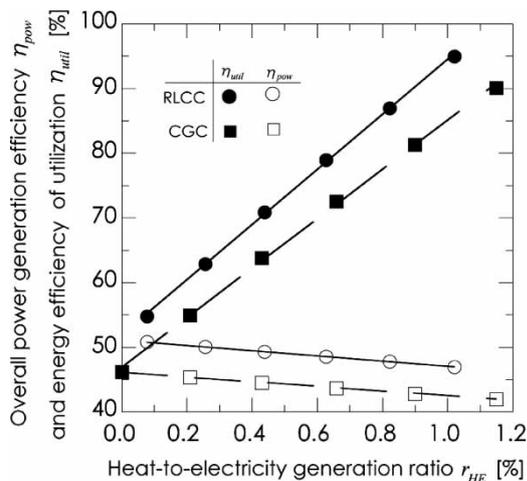
higher than that of the CGC system. The highest η_{util} of the RLCC system is 95.0 per cent, and it is 91.0 per cent for the CGC system.

Due to some safety concerns with the fuel preheat in the recuperator, mentioned in section 1, the effect of eliminating fuel preheating on system performance was computed for an RLCC system that does not employ fuel preheating, at TP = 2.0 MPa, TIT1 = 1623 K. It was found that the elimination of fuel preheating caused the power generation efficiency of the topping GT cycle to drop by 0.5 percentage points, from 36.8 to 36.3 per cent, the overall power generation efficiency by 0.3 percentage points, from 50.6 to 50.3 per cent, while the energy efficiency of utilization remained at 95.0 per cent. This indicates that the fuel preheating can be eliminated with insignificant impact on system performance.

As stated at the outset, one of the main objectives for developing the RLCC system is the reduction of NO_x emissions. Although reliable prediction of these emissions requires complete knowledge of the combustor configuration and flow and transport fields, which obviously are not available at this stage of the system development, the least that can be done now is to use the Gibbs free energy model described section 3.2. Use of this model tends to over-estimate the NO_x emissions, so the computed values constitute a conservative estimate. Table 9 presents the computed results, emissions on a power basis, compared with those from the CGC system, at the conditions of the highest power generation efficiency. There are two obvious reasons why the proposed RLCC system reduces the overall power-based NO_x emissions: (a) as can be seen from Table 8, the exhaust mass flow decreases, (b) the power generation efficiency increases, and (c) NO_x emissions from CB1 are affected only slightly by the higher TIT1 because of the fuel-rich conditions there. In the proposed RLCC system the emissions decrease as the turbine inlet temperature at GT1 and top pressure of the system rise; at TIT1 = 2073 K the emissions from the proposed system are 34 per cent lower than those from the CGC system, indicating that the proposed system is a more environmentally friendly energy conversion system.

The predicted efficiency and emissions advantages of the proposed RLCC system must of course be evaluated against possible increased equipment costs, and possible decreased plant availability related to reliability. Although it is impossible at this stage of a novel system to predict the latter, a rough comparison of the RLCC and CGC systems can be made. They differ primarily in the fact that (a) the former has a high temperature turbine with C/C composite blades and it is impossible to estimate the cost of turbines, which are not yet in production (although, if the material is proven to be successful in long term operation

Fig. 9 Relationship between the heat-to-electricity generation ratio (r_{HE}) and efficiencies of the RLCC system (TIT1 = 1623 K, TP = 2.0 MPa) and the CGC system (TIT = 1623 K, TP = 2.0 MPa)

Table 9   Overall power generation efficiency and NO$_x$ emissions on power generation basis (TIT, turbine inlet temperature; TP, top pressure of the system; η_{pow}, overall power generation efficiency)

	RLCC system			CGC system
	TIT1 = 1623 K, TP = 2.0 MPa	TIT1 = 1623 K, TP = 4.0 MPa	TIT1 = 2073 K, TP = 4.0 MPa	TIT1 = 1623 K, TP = 2.0 MPa
Overall power generation efficiency, η_{pow} (%)	50.6	51.7	53.0	44.4
NO$_x$ emissions, (mg/s-kW)	4.21	3.856	3.21	5.01

the cost should not be much different than conventional turbines) and (b) they require a different heat exchanger area. We have thus evaluated the total area of the heat exchangers (IC, RE, and SG) for both systems. The heat exchanger area A is a function of the overall heat-transfer coefficient U as related by

$$UA = \sum_{IC,RE,SG} Q/\Delta T_{lm} \tag{12}$$

where ΔT_{lm} is the overall log mean temperature difference (LMTD) defined as

$$\Delta T_{lm} = \frac{(T_{hot,out} - T_{cold,in}) - (T_{hot,in} - T_{cold,out})}{\ln[(T_{hot,out} - T_{cold,in})/(T_{hot,in} - T_{cold,out})]} \tag{13}$$

Table 10 contains the comparisons of the heat-transfer coefficient and area product, UA, as well as the specific UA per unit generated power, $UA/(W_{GT} + W_{SP} - W_{CP})$. The result shows that this specific UA of the RLCC system is smaller than that of the CGC system by about 32 per cent. This result is explained for the reasons already stated; the high power generation efficiency (η_{pow}) and low mass flowrates of the air and fuel ($m_{fuel} + m_{air}$) of the RLCC system compared with the CGC system. The costs of the other components excluding the GT1, that is GT2, ST, SG, and IC, will be of the same order for both systems because they are similar.

Assuming that the novel turbine GT1 would be successful and of cost similar to conventional high temperature gas turbines (following ongoing development at Nagoya University and elsewhere [**14**, **15**, **18**]),

these results indicate that the RLCC has better performance at what is probably about the same cost as the conventional CGC.

6   SUMMARY AND CONCLUSIONS

This article proposes, describes, and analyses a novel advanced reheat cogeneration system based on a two-stage fuel-rich fuel-lean (RLCC) system and compares its performance with a CGC system. Since typically the highest exergy loss is in the combustion process, the advantages of the proposed staged combustion are estimated by conducting an exergy analysis of this system in comparison with a conventional two-stage (fuel-lean fuel-lean) combustion process. The proposed fuel-rich/fuel-lean combustion reduces the exergy loss in the combustor by about 2.0 percentage points.

A thermodynamic analysis of the RLCC system shows that it may have an overall power generation efficiency up to 53.0 per cent (LHV basis), an exergy efficiency up to 61.9 per cent, and specific power up to 524.3 kJ/kg. The exergy analysis confirms that the dominant exergy loss is in the combustion process. In the RLCC system this loss is 22.8 per cent at TIT1 = 2073 K and TP = 2.0 MPa, whereas it is 25.0 per cent in the CGC system at TIT1 = 1623 K and TP = 2.0 MPa. The energy utilization efficiency of the RLCC system was found to be as high as 95.0 per cent, 4.0 percentage points higher than that of the CGC system. The overall power-based NO$_x$ emissions from the RLCC system are up to 36 per cent lower than those from the CGC system.

A very rough estimate of the cost of the components in the proposed RLCC system relative to a CGC indicates that the cost of all the components except the yet unknown high temperature GT (GT1) should at worst be the same, and at best lower, since the heat exchanger area per unit generated power is about 32 per cent lower.

To put the RLCC system to practice, more research is needed on the development and use of turbine blades that can withstand these higher temperatures, such as those made of the C/C composites, and on

Table 10   Function of the overall heat-transfer coefficient and the heat-transfer area, UA (TIT, turbine inlet temperature; TP, top pressure of the system; W_{CP}, compressor work; W_{GT}, W_{ST}, GT and ST power)

	RLCC (TIT1 = 1723 K, TP = 2.0 MPa)	CGC (TIT = 1723 K, TP = 2.0 MPa)
UA (kJ/(K s)	78.01	100.56
$(W_{GT} + W_{SP} - W_{CP})$ (kW)	2695	2367
$UA/(W_{GT} + W_{SP} - W_{CP})$ (1/K)	2.89×10^{-2}	4.24×10^{-2}

high-pressure and high-temperature fuel-rich combustion. In work published elsewhere, the authors and their co-workers have developed coating techniques for C/C composites [**18**] and obtained encouraging experimental results on the methods developed for reducing soot formation in fuel-rich combustion [**24**, **25**].

REFERENCES

1 **Oh, S.-D., Pang, H.-S.,** and **Yong, K.-H.** Exergy analysis of a gas turbine cogeneration system. *ASME, J. Eng. Gas Turbines Power*, 1996, **118**(4), 253–260.

2 **Mori, A., Nakamura, H., Takahashi, T.,** and **Yamamoto, K.** A highly efficient regeneration gas turbine system by new method of heat recovery with water injection. Tokyo International Gas Turbine Congress, 1983, vol. 1, pp. 45–51.

3 **Penning, F. M.** and **De Lang, H. C.** Steam injection: analysis of a typical application. *Appl. Therm. Eng.*, 1996, **16**(2), 115–125.

4 **Najjar, Y.** and **Zaamout, M.** Enhancing gas-turbine engine performance by means of the evaporative regenerative cycle. *Energy*, 1996, **69**, 2–8.

5 **Waldyr, G.** Comparison between the HAT cycle and other gas turbine based cycles: efficiency, specific power and water consumption. *Energy Convers. Manage.*, 1997, **38**(15–17), 595–1604.

6 **Kim, T. S., Song, C. H., Ro, S. T.,** and **Kauh, S. K.** Influence of ambient condition on thermodynamic performance of the humid air turbine cycle. *Energy*, 2000, **25**(4), 313–324.

7 **Yunhan, X., Ruixian, C.,** and **Rumou, L.** Modeling HAT cycle and thermodynamic evaluation. *Energy Convers. Manage.*, 1997, **38**(15–17), 1605–1612.

8 **Saad, M. A.** and **Dah, Y. C.** The new LM2500 Cheng cycle for power generation and cogeneration. *Energy Convers. Manage.*, 1997, **38**(15–17), 1637–1646.

9 **Nakhamkin, M.** and **Potashnik, B.** Humidified air injection raises peak turbine output. *Power Eng.*, 1999, **1**, 80–86.

10 **Arai, N.** and **Kobayashi, N.** Challenges for development of highly efficient gas turbine system: the chemical gas turbine system. In Proceedings of Joint Power Generation Conference '97, Denver, USA, 1997, vol. 1, pp. 423–429.

11 **Lior, N.** and **Arai, N.** Performance and heat transfer considerations in the novel chemical gas turbine system. In Proceedings of AIAA/ASME Joint Thermophysics and Heat Transfer Conference '98, Albuquerque, USA, 1998, vol. 4, pp. 33–39.

12 **Yamamoto, T., Furuhata, T., Arai, N.,** and **Mori, K.** Thermodynamic analysis and optimization of new concept combined cycle "chemical gas turbine" system. In Proceedings of International Symposium on Efficiency, Costs, Optimization, and Environmental Aspects of Energy Systems, Enschede, The Netherlands, 2000, vol. 1, pp. 447–455.

13 **Yamamoto, T., Furuhata, T., Arai, N.,** and **Lior, N.** Analysis of a high-efficiency low-emissions "chemical gas turbine" system. *AIAA J. Propuls. Power*, 2002, **18**(2), 432–439.

14 **Fushitani, K., Kobayashi, N.,** and **Arai, N.** Evaluation of high temperature oxidation behavior of carbon-carbon composites exposed in a field of combustion by using raman spectroscopy. *J. Chem. Eng. Japan*, 1997, **30**, 580–582.

15 **Kato, Y., Kakamu, K., Hironaka, Y., Arai, N., Kobayashi, N.,** and **Pierre, G. R. S.** Improvement of high-temperature endurance of C/C composites by double coating with SiC and glass materials. *J. Chem. Eng. Japan*, 1996, **24**(4), 669–674.

16 **Yamamoto, T., Kobayashi, N., Arai, N.,** and **Tanaka, T.** Effect of pressure on fuel-rich combustion of methane–air under high pressure. *J. Energy Convers. Manage.*, 1997, **38**(10–13), 1093–1100.

17 **Kobayashi, N., Mano, T.,** and **Arai, N.** Fuel-rich hydrogen-air combustion for a gas turbine system with no emission of carbon dioxide. *Energy*, 1997, **22**, 189–197.

18 **Kato, Y., Kakamu, K., Hironaka, Y.,** and **Arai, N.** Improvement of high-temperature endurance of C/C composites by double coating with SiC and glass materials. *J. Chem. Eng. Japan*, 1997, **30**(3), 580–582.

19 **Kozu, M.** and **Tsuruno, S.** Exergy analysis of combined cycle using T–S diagram. *J. Gas Turbine Soc. Japan*, 1994, **22**(87), 64–72.

20 **Dunbar, W. R.** and **Lior, N.** Sources of combustion irreversibility. *Combust. Sci. Technol.*, 1994, **103**, 41–61.

21 **Lior, N.** Irreversibility in combustion. In Proceedings of Efficiency, Costs, Optimization, Simulation and Environmental Aspects of Energy System, Istanbul, Turkey, 2001, vol. 1, pp. 39–48.

22 **Brandauer, M.** GT26 repowers Rheinhafen. *Fuel Energy Abstr.*, 1996, **37**(5), 373.

23 **Harvey, S.** and **Kane, N. D.** Analysis of a reheat gas turbine cycle with chemical recuperation using Aspen. *Energy Convers. Manage.*, 1997, **38**(15–17), 1671–1679.

24 **Ochi, T., Kishi, N., Furuhata, T.,** and **Arai, N.** Effect of H_2 addition on soot formation in fuel-rich CH_4/air turbulent diffusion flame. In Proceedings of International Joint Power Generation Conference, San Francisco, USA, 2002, vol. 3, pp. 122–129.

25 **Kishi, N., Ochi, T., Furuhata, T.,** and **Katagiri, H.** Soot formation in fuel-rich methane/air diffusion flame. In Proceedings of first International Energy Conversion Engineering Conference, Portsmouth, USA, 2003, vol. 1, pp. 43–49.

26 **Yamamoto, T.** *A study for chemical and thermal energy conversion processes in the turbine system*. PhD Thesis, Nagoya University, 2002.

27 **Gorden, S.** and **McBride, B. J.** Computer program for calculation of complex equilibrium composition, rocket performance incident and reflected shocks and chapman-jouget detonation. NASA Technical Report, SP-273, 1971.

28 HYSYS ver.1.1. *Reference book*, vol. 1–2, 1997 (Hyprotech Co., Calgary, Canada).

APPENDIX

Nomenclature

E	exergy (W)
H	enthalpy (W)
m	mass flowrate (kg/s)
MP	medium pressure of the RLCC system (Pa)
P	pressure (Pa)
Q	heat (W)
r_{HE}	heat-to-electricity generation ratio, equation (11)
S	entropy (W/K)
SP	specific power, equation (7) (J/kg)
T	temperature (K)
TP	top pressure of each system (Pa)
TIT1	turbine inlet temperature of first GT in the RLCC system (K)
TIT2	turbine inlet temperature of second GT in the RLCC system (K)
TOT1	turbine outlet temperature of first GT in the RLCC system (K)
TOT2	turbine outlet temperature of second GT in the RLCC system (K)
U	overall heat-transfer coefficient (W/m^{2}K)
W	work (W)

ΔP	pressure drop (Pa)
η_{ex}	exergy efficiency, equation (9)
η_{GT-pow}	power generation efficiency of topping GT cycle, equation (6) (%)
η_{pow}	overall power generation efficiency, equation (8) (%)
η_{util}	energy utilization efficiency, equation (10) (%)
ϕ	equivalence ratio

Subscripts

air	air
burn	burning state
c	cold stream
CP	compressor
ex	exergy
fuel	fuel
GT	gas turbine
h	hot stream
in	inlet state
mix	mixing state
out	outlet state
P	pump
stoich	stoichiometric condition
ST	steam turbine
0	ambient state